

Temperature dependence of the exciton gap in monocrystalline CuGaSe₂

This article has been downloaded from IOPscience. Please scroll down to see the full text article.

2003 J. Phys.: Condens. Matter 15 6219

(<http://iopscience.iop.org/0953-8984/15/36/310>)

View [the table of contents for this issue](#), or go to the [journal homepage](#) for more

Download details:

IP Address: 171.66.16.125

The article was downloaded on 19/05/2010 at 15:09

Please note that [terms and conditions apply](#).

Temperature dependence of the exciton gap in monocrystalline CuGaSe₂

A Meeder^{1,4}, A Jäger-Waldau², V Tezlevan³, E Arushanov³,
T Schedel-Niedrig¹ and M Ch Lux-Steiner¹

¹ Hahn-Meitner Institut GmbH, Glienicker Straße 100, D-14109 Berlin, Germany

² EC, DG-JRC, IES-Renewable Energies Unit, Ispra, Italy

³ Institute of Applied Physics, Academy of Sciences of Moldova, Kishinev, MD 2028, Moldova

E-mail: meeder@hmi.de

Received 1 April 2003, in final form 5 August 2003

Published 29 August 2003

Online at stacks.iop.org/JPhysCM/15/6219

Abstract

Near-band-edge photoluminescence properties of as-grown undoped CuGaSe₂ single crystals have been investigated in the range between 10 K and room temperature. The temperature dependence of the exciton gap energy E_g was studied by means of a three-parameter thermodynamic model, the Einstein model, Varshni's model and the Pässler model. The values of the band gap energy at $T = 0$ K, the effective phonon energy and the Einstein temperature, the cut-off phonon energy of the phonon spectrum as well as a dimensionless constant related to the electron–phonon coupling were estimated. Comparing all applied models points out that a minimum set of four parameters is required for a complete analytical description of the experimentally determined temperature dependence of the exciton gap in CuGaSe₂.

1. Introduction

CuGaSe₂ is promising for use in red-light-emitting devices, light detectors, and as an absorber material in solar cells. So far, CuGaSe₂-based solar cells with a CdS buffer have achieved efficiencies of 9.3 and 9.7% as thin-film [1] and single-crystal [2] solar cells, respectively. This is considerably lower than for Cu(In, Ga)Se₂ solar cells. However, CuGaSe₂ shows some theoretical advantages with respect to module integration due to its higher band gap. Furthermore, a tandem arrangement of CuInSe₂ and CuGaSe₂ could increase the device efficiency above 33% [3]. Photoluminescence spectroscopy is a widely used method to determine the value of the band gap energy E_g , as well as for the identification of the fundamental defects and impurity levels of a semiconductor. Several photoluminescence studies on CuGaSe₂ single crystals [4–7] and layers have been published [7–13]. However, the

⁴ Author to whom any correspondence should be addressed.

value of E_g and its temperature dependence have not been well determined up to now. In earlier publications a maximum of $E_g(T)$ was reported in the range 50–100 K, while more recently published low-temperature $E_g(T)$ studies on CuGaSe₂ single crystals, grown by the gradient freezing method, and epitaxial films, grown on GaAs, do not show such anomalous behaviour of the band gap energy as a function of temperature [7]. The temperature variation of E_g in the range between 10 and 160 K [9, 14], as well as the variation of the photoluminescence peak energy (PE) position versus T , have been determined and fitted using the Manoogian–Wolley [14] equation. However, with five parameters to fit, the reliability of the results is limited [15].

In this study we report on excitation intensity and temperature-dependent, steady-state photoluminescence measurements on CuGaSe₂ single crystals grown by chemical vapour transport (CVT). CuGaSe₂ (CGSe) single crystals are used as a reference system to get more reliable data on the physical properties of the material of interest and its parameters excluding the effects of substrate stress and extrinsic doping due to diffusion (likely in thin films on foreign substrates). The value of the exciton gap is determined from luminescence measurements and its variation with temperature is studied using Varshni's empirical model [16], a thermodynamic model of O'Donnell and Chen [15], the Einstein model [17] and the Pässler model [18]. Therefore, we briefly summarize the physical bases of the four models.

First, approximating the two basic features of experimentally observed $E_g(T)$ curves—an almost quadratic dependence at low temperatures and a linear dependence at high temperatures—Varshni suggested equation (1), an empirical description of the $E_g(T)$ dependence [16]:

$$E_g(T) = E_g(0) - \alpha T^2 / (T + \beta). \quad (1)$$

$E_g(0)$ represents the band gap at zero temperature, $-\alpha$ the $(T \rightarrow \infty)$ limit of $dE_g(T)/dT$, and β is a temperature parameter.

Second, it is well known that both the thermal dilation of the lattice and the electron–phonon interaction will contribute to the temperature variation of the band gap energy. For many semiconductors the first component can usually be neglected due to its limited contribution. Hence the electron–phonon coupling is dominant and can be described by a three-parameter thermodynamic model [15]:

$$E_g(T) = E_g(0) - S \langle E_{\text{ph}} \rangle [\coth(\langle E_{\text{ph}} \rangle / 2k_B T) - 1], \quad (2)$$

where $E_g(0)$ is the band gap at $T = 0$ K, $\langle E_{\text{ph}} \rangle$ is an effective phonon energy, and S is a dimensionless constant related to the electron–phonon coupling. Equation (2) provides a good description of $E_g(T)$ for various semiconducting materials such as Si, GaAs, GaP, diamond, β -FeSi₂ [15, 19] and InP_{*x*}As_{1–*x*} [20].

Third, using the Einstein model, the $E_g(T)$ dependence can be expressed by the following equation [17]:

$$E_g(T) = E_g(0) - K (e^{\Xi/T} - 1)^{-1}, \quad (3)$$

where K is a temperature-independent constant and Ξ is the Einstein temperature. The physical basis for equation (3) is the Einstein representation of the total thermal energy of the solid. Based on the equality $\coth(x/2) - 1 = 2/(\exp(x) - 1)$, Pässler [18] showed the identity of the independently found empirical model equations (2) and (3) simply, defining $x = \langle E_{\text{ph}} \rangle / k_B T$. Then equation (2) can be rewritten in the following manner:

$$E_g(T) = E_g(0) - (2S \langle E_{\text{ph}} \rangle) / (\exp \langle E_{\text{ph}} \rangle / k_B T - 1). \quad (4)$$

Equation (4) represents the Einstein model (3) with the Einstein temperature $\Xi = \langle E_{\text{ph}} \rangle / k_B$ and the constant $K = 2S \langle E_{\text{ph}} \rangle$.

Fourth, Pässler [18] proposed an analytical description of E_g versus T within the regime of dominant electron–phonon interaction. According to this theory, the variation can be expressed by

$$E_g(T) = E_g(0) - \int f(\varepsilon)n(\varepsilon, T) d\varepsilon, \quad (5)$$

where ε is the phonon energy, $n(\varepsilon, T) = [\exp(\varepsilon/k_B T) - 1]^{-1}$ represents the average phonon occupation number, and $f(\varepsilon)$ is the relevant electron–phonon spectral function, which is given by a power-law dependence of the form $f(\varepsilon) \propto \varepsilon^\eta$ within the energy range of 0 eV up to a cut-off value of $\varepsilon_c = [(\eta + 1)/\eta]k_B\Theta$. For exponents within a range of $1.2 < \eta < 1.6$, which corresponds to a moderately concave spectral function, equation (5) can be simplified to [18]:

$$E_g(T) = E_g(0) - \delta \frac{\Theta}{2} \{ [1 + (2T/\Theta)^p]^{1/p} - 1 \}, \quad (6)$$

where $-\delta$ is equal to the high-temperature limit of $dE_g(T)/dT$, Θ is the effective phonon temperature (expected to be smaller than the Debye temperature, $2\theta_D/3$ [18] or $\Theta \approx 3\theta_D/4$ [21]), and the parameter $p = \eta + 1$. The exponent η governs the shape of the spectral function.

While the first three models comprise only three empirical parameters, the Pässler model comprises four empirical parameters. The results are discussed in the framework of Pässler's finding [18] that a minimum set of four parameters is a necessary condition for any analytical description of the $E_g(T)$ dependence of different semiconductor materials.

2. Experiment

Single crystals were grown by CVT in a closed system using iodine as a transport agent. The polycrystalline material, preliminary synthesized in iodine atmosphere at a temperature of about 800 °C from a stoichiometric mixture of the elemental constituents, was used as the raw charge in the CVT. The iodine concentration was approximately 5 mg cm⁻³. The source temperature and the growth temperature were about 850 and 780 °C, respectively. The monocrystallinity of the crystals was proved by applying the Laue x-ray diffraction method. Photoluminescence spectra were obtained between 10 K and room temperature using the 514.5 nm emission line of a cw Ar⁺ laser (Coherent Innova 90) as the excitation source. The excitation intensity was varied between 10 mW cm⁻² and 100 W cm⁻² by using neutral density filters. The luminescence was spectrally analysed by a 0.22 m grating monochromator (SPEX 1680) and a liquid-nitrogen-cooled photomultiplier (Hamamatsu R3236). The spectral resolution for the measurement of the excitonic luminescence lines was $\lambda/\Delta\lambda = 1000$.

3. Results and discussion

Figure 1 shows a plot of the typically observed luminescence spectrum of a nearly stoichiometric CVT-grown CGSe single crystal at $T = 10$ K and $P_{\text{exc.}} = 20$ mW. Two peaks above 1.6 eV dominate the spectrum, while the low-energy region exhibits no luminescence. The first peak ($h\nu \approx 1.724$ eV) can be correlated with free excitonic (FX) and bound excitonic (BX) transitions (see inset). The non-symmetric peak shape is well fitted by using two Gaussians, each with a FWHM of 3 meV and a separation of 4 meV. According to the power law $I \sim p_{\text{laser}}^k$, both peaks show a super-linear dependence of their PL intensity on excitation power density ($k_{\text{FX}} = 1.5$, $k_{\text{BX}} = 1.4$). A k -factor between 1 and 2 is a main characteristic of excitonic luminescence when exciting with photon energies far beyond the band gap [22].

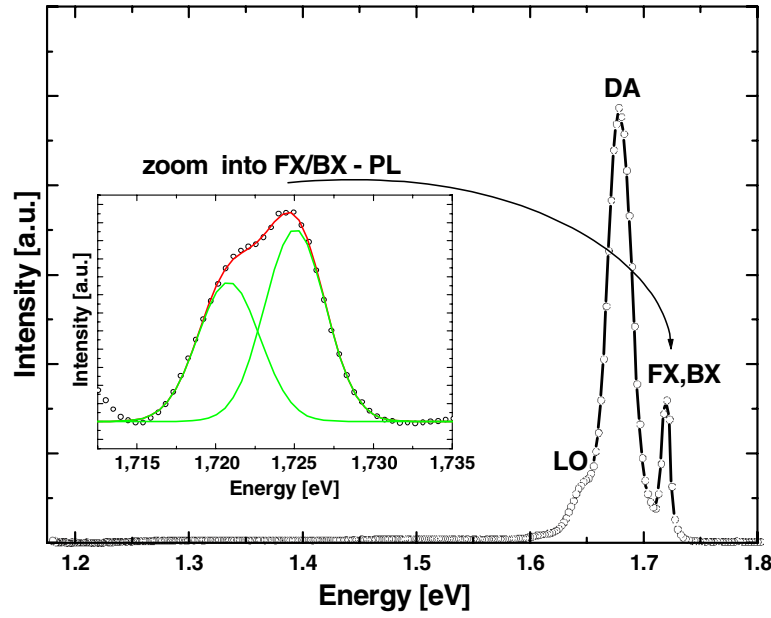


Figure 1. A PL-spectra overview of a CuGaSe₂ single crystal at 10 K and high-resolution spectra of BX and FX luminescence (inset, open circles). Solid curves represent Gaussian fits to the data. (This figure is in colour only in the electronic version)

Similar values for the k -factor, line-shape, FWHM and peak position for the close-to-band-edge luminescence of nearly stoichiometric CGSe have been reported elsewhere [7, 9]. These authors attribute the observed features to a free exciton and a bound exciton, in our case located at $h\nu_{(\text{FX})} = 1.725$ eV and $h\nu_{(\text{BX})} = 1.721$ eV. Experimental and theoretical data for the free-exciton binding energy $E_{(\text{FX})}$ vary between 13 and 17 meV [7, 9]. Using the smallest value, we estimate a band gap energy at 10 K of $E_g = h\nu_{(\text{FX})} + E_{(\text{FX})} = 1.738$ eV. The most intense PL peak at 1.674 eV can be identified as a donor–acceptor (DA) pair transition (see the details in [23]). The low-energy shoulder of the DA transition, located (34 ± 2) meV lower in energy, is attributed to a phonon replica of the DA transition [12, 13, 23].

We conclude that, despite the general observation of slightly higher transition energies (about 10 meV), we found excellent agreement with most recent PL studies on stoichiometric 1:1:2 CGSe films and crystals (for details, see [7, 12, 13, 23]).

The temperature dependence of the near-band-edge photoluminescence was studied further in the range from 10 to 300 K. Exemplary spectra of the temperature series are shown in figure 2. Such luminescence studies have been performed by various authors [7–9]. While the observed spectra shown in these publications are in good agreement with our data, the interpretation of the specific type of transition seems to be somewhat tricky. An overall decrease of the luminescence intensity (not shown here) with increasing temperature can be attributed to a change of the dominant recombination mechanism, namely from radiative to non-radiative recombination. Alterations in the near-band-edge luminescence peak structure must be considered in terms of different radiative recombination paths. One can expect a change from excitonic to band–band (BB) luminescence with increasing temperature. Such a change in the dominant radiative recombination path would result in luminescence at an energy [24] of $h\nu_{(\text{BB})} = E_g + (k_B T/2)$. Therefore, the transition energies of the free-exciton

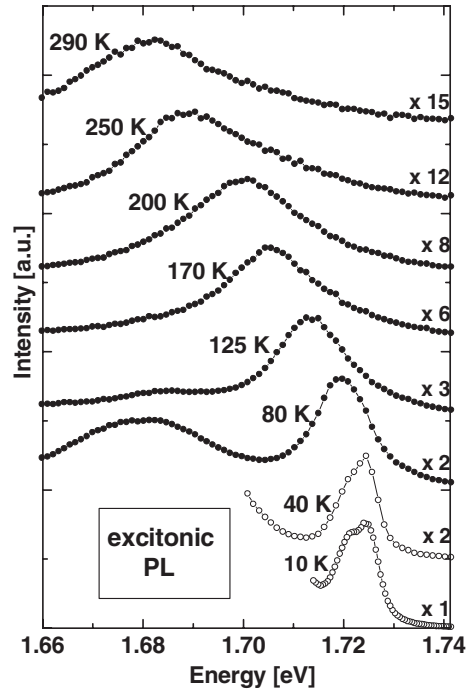


Figure 2. A near-band-edge PL spectra series of a CuGaSe₂ single crystal in the temperature range between 10 and 300 K.

($h\nu_{(\text{FX})}$) and the band–band ($h\nu_{(\text{BB})}$) luminescence would be separated by $E_{(\text{FX})} + k_{\text{B}}T/2$. At around 150 K the thermal energy of the system equals the binding energy of the free exciton. Therefore, we expect an additional high-energy luminescence signal in the high-temperature spectra of figure 2. As is shown, no new luminescence feature appears in the spectra series with increasing temperature. Instead, the near-band-edge luminescence signal, identified at 10 K as free-excitonic luminescence, shifts linearly with increasing temperature to lower energies. Our PL data therefore support the interpretation of near-band-edge luminescence dominated by excitonic states even at room temperature. This interpretation is in agreement with piezoelectric photoacoustic PPA measurements of Yoshino *et al* [14]. The broad and asymmetric structure of the high-energy peak side, found at temperatures above 150 K, is likely to be due to a mixture of band-to-band tail and band-to-band luminescence. Band tail transitions, even in stoichiometric CGSe, are the focus of some recent studies [25].

The peak energy variation with temperature, $PE(T)$, of the near-band-edge luminescence was analysed further using the empirical model of Varshni (1), the thermodynamic model of O’Donnell and Chen (2) as well as the Einstein model (3) and the Pässler model (6)—see figure 3. Assuming that the band gap energy can be obtained simply by adding the free-exciton binding energy to the $PE(T)$ data over the whole temperature range, we exchanged $E_{\text{g}}(T)$ with the transition energy of the near-band-edge photoluminescence $PE(T)$, i.e. the free-exciton transition energy, and the fit parameter $E_{\text{g}}(0)$ in all four models (equations (1)–(3) and (6)) with $PE(0)$. All four fitting plots are within the experimental error of the data, as shown in figure 3. Especially at the high-temperature side, where the experimental data approach the asymptotic $T \rightarrow \infty$ limit (dotted straight line, figure 3), all fittings become equal. Nevertheless, slight differences can be seen in the low-temperature regime, as shown in the inset of figure 3.

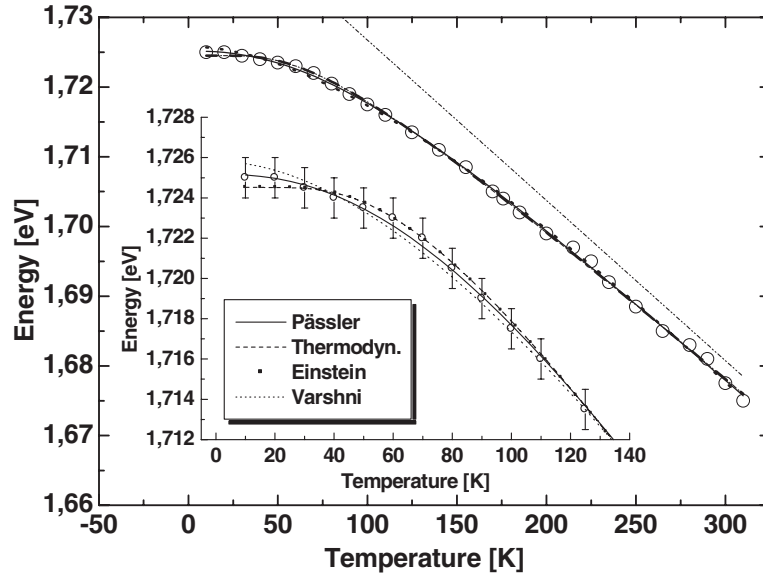


Figure 3. The temperature dependence of the peak energy of near-band-edge luminescence, $PE(T)$, in CuGaSe_2 . The open circles are the experimentally obtained peak energies (PE), the curves (see inset for the low-temperature $PE(T)$ region) represent the calculated dependency according to (a) the Varshni model (dotted curve), (b) the thermodynamic model (dashed curve), (c) the Einstein model (black dots), and (d) the Pässler model (straight line). The dotted line in the main plot is a guide to the eye, indicating the $(T \rightarrow \infty)$ asymptote of $PE(T)$.

Table 1. Values of the adjustable parameters $(PE(0), \alpha, \beta)$, $(PE(0), \langle E_{\text{ph}} \rangle, S)$, $(PE(0), K, \Xi)$ and $(PE(0), \delta, \Theta, p)$, obtained by fitting equations (1)–(3) and (5), respectively, to the temperature dependence of peak energies of near-band-edge luminescence (PE) data of CuGaSe_2 . The errors in these parameters are given in parentheses below the corresponding value.

	Equation (1)			Equation (2)			
	$PE(0)$ (eV)	α (meV K ⁻¹)	β (K)	$PE(0)$ (eV)	$\langle E_{\text{ph}} \rangle$ (meV)	S	
$PE(T)$	1.7258 (0.0002)	0.29 (0.01)	244 24	1.7245 (0.0002)	18 (0.7)	1.29 (0.02)	
	Equation (3)			Equation (6)			
	$PE(0)$ (eV)	K (eV)	Ξ (K)	$PE(0)$ (eV)	δ (meV K ⁻¹)	Θ (K)	p
$PE(T)$	1.7245 (0.0002)	0.046 (0.002)	208 (8)	1.7252 (0.0002)	0.23 (0.01)	215 (26)	2.3 (0.2)

While Varshini's models leads to a slight overestimation of the $PE(T)$ data, both the thermodynamic and the Einstein model underestimate the low-temperature $PE(T)$ data. As predicted theoretically, a perfect match of the latter two models is observed. Finally, the Pässler model shows the best fit to the data.

The obtained fitting parameters are summarized in table 1. The resulting material properties will be discussed briefly in the following.

By fitting equation (2) to our data of $PE(T)$, the following set of parameters was obtained: $PE(0) = 1.7245 \pm 0.0002$ eV, $S = 1.29 \pm 0.02$, and $\langle E_{\text{ph}} \rangle = 18 \pm 1$ meV—see table 1.

Our value of the electron–phonon coupling parameter S is lower than the reported value for Si (1.49) [15] and III–V compounds like InP (1.94) [20], GaAs (3.0) and GaP (3.35) [15]. It can be concluded that the interaction between band-edge states and the phonon system in CuGaSe₂ is not as strong as in silicon, indium or gallium phosphides and arsenides.

Further, from equations (2) or (3) we can write

$$\frac{dPE}{dT} = -\frac{S\langle E_{\text{ph}}^2 \rangle}{2kT^2 \sinh^2(\langle E_{\text{ph}} \rangle / 2k_B T)}. \quad (7)$$

At high temperatures, $k_B T \gg \langle E_{\text{ph}} \rangle$, the slope of the $PE(T)$ curve approaches its limiting value:

$$-\left[\frac{dPE}{dT}\right]_{\text{max}} = 2Sk_B. \quad (8)$$

Comparing the above given $T \rightarrow \infty$ asymptote of equations (2) or (3) with its counterpart due to equation (6), the following correlations between the different model parameter are found: $2Sk_B = K/\Xi = \delta$ for the magnitude of the limiting slope and $\langle E_{\text{ph}} \rangle / k_B = \Xi = \Theta$ for the effective phonon temperature. Comparing the parameter values listed in table 1, we conclude that, within deviations of less than 5%, these theoretical relations are fulfilled.

The calculated value of $-(dPE/dT)_{\text{max}} = 0.22$ meV K⁻¹ is close to the parameters $\alpha = 0.29$ meV K⁻¹ obtained by Varshni's model and $\delta = 0.23$ meV K⁻¹ obtained by the Pässler model. The value of $-(dPE/dT)$ decreases with decreasing temperature ($-(dPE/dT) = 0.219$ meV K⁻¹ at room temperature, 0.188 meV K⁻¹ at 150 K and 0.149 meV at 100 K, obtained using the Pässler fit). Reported values of $-(dE_g/dT)$ vary from 0.11 [5] (in the range 40–200 K) up to 0.20–0.21 meV K⁻¹ [7, 26] (between 100 and 300 K).

Assuming that mobility μ is determined by lattice scattering, its value can be expressed by [19]

$$\mu = \frac{48}{9\pi} \left(\frac{3}{4\pi}\right)^{1/3} \left(\frac{\pi}{2}\right)^{1/2} \frac{e\hbar^2 k}{(\Omega)^{1/3} m^{*3/2} (k_B T)^{3/2} (dE_g/dT)} \quad (9)$$

where Ω is the volume of the unit cell and m^* is the effective mass. The hole mobility was calculated by assuming that $(dPE/dT) = (dE_g/dT)$ and that the ratio of hole mass to electron mass $m_h/m_e = 1.2$ [4]. At room temperature we estimate a hole mobility of $\mu = 43$ cm² V⁻¹ s⁻¹ (by applying the thermodynamic model and the Einstein model), 45 cm² V⁻¹ s⁻¹ (by applying Pässler's model) and 47 cm² V⁻¹ s⁻¹ (by applying Varshni's model). All values are slightly higher but close to previously reported data for the room-temperature Hall mobility value obtained on similarly grown CVT single crystals (20–30 cm² V⁻¹ s⁻¹) [4] as well as polycrystalline thin films grown on (slg) glass substrates (10–20 cm² V⁻¹ s⁻¹) [27], while room-temperature Hall mobility data obtained on epitaxially grown CGSe/GaAs(001) show considerably higher values (100–170 cm² V⁻¹ s⁻¹) [28].

It should be mentioned that equation (6) provides a rather good approximation of equation (5), particularly for the parameter range $p \approx 2.2$ – 2.6 . This restrictive requirement is valid for the case of our CGSe data. By fitting equation (6) to our data of $PE(T)$, the following set of parameters is obtained: $PE(0) = 1.7252 \pm 0.0002$ eV, $\Theta = 215 \pm 26$ K, $p = 2.3 \pm 0.2$, and $\delta = 0.23 \pm 0.01$ meV K⁻¹—see table 1. An effective phonon energy $k_B \Theta$ is equal to 19 ± 1 meV. A cutoff phonon energy is found to be 33 ± 2 meV. At room temperature, Rincon and Ramirez [29] have reported on nine optical phonon modes in CuGaSe₂

by means of Raman spectroscopy. The frequencies of these modes vary from the lowest value at 60 cm^{-1} (7 meV) up to the highest value at 273 cm^{-1} (34 meV). Using infrared reflectivity spectroscopic data, Bodnar *et al* [30] report on eight optical phonon modes in CuGaSe_2 . The frequencies of these modes vary from the lowest value at 170 cm^{-1} (21 meV) to the highest value at 278 cm^{-1} (34 meV). The cutoff phonon energy, as estimated from the Pässler model, is close to the highest frequency modes observed in the Raman and IR investigations, and the difference is within the accuracy of the data. Further, the cutoff energy is close to the experimentally determined energy separation of the observed LO-phonon replica of the DA transition ($34 \pm 2\text{ meV}$).

We can conclude that, in comparison with the three-parameter models, the four-parameter Pässler model shows the best overlap between estimated data from the fitting parameters, experimental data and data in the literature. Nevertheless, all models are good enough to fit the experimental data within the accuracy of the measurement.

It was found that the low-temperature value of the peak energy of near-band-edge luminescence is somewhat higher for less stress due to the influence of the substrate on the CuGaSe_2 growth. It reaches up to about 1.720 eV in unstrained films [11] and 1.728 eV in single crystals [7]. The high value of PE observed in our samples (1.7252 eV, Pässler model—table 1) confirms the high quality of the crystals studied. Adding a minimum free-exciton binding energy of 13 meV, the minimum band-gap energy at $T = 0\text{ K}$ is estimated to be 1.7382 eV and, thus, it is higher than recently reported values (1.7305 [5], 1.7347 [6], 1.731 eV [14]).

4. Conclusions

Photoluminescence properties of as-grown undoped CuGaSe_2 single crystals have been investigated in the temperature range between 10 and 300 K. The temperature dependence of the near-band-edge PL, reflecting the temperature dependence of the excitonic band gap energy E_g , was studied by means of the Varshni model, a three-parameter thermodynamic model, the Einstein model, and the Pässler model. The values of the band gap at $T = 0\text{ K}$, an effective and a cut-off phonon energy, a dimensionless constant related to the electron–phonon coupling and an estimation for the room-temperature hole mobility of CGSe, have been derived from the applied models. While all applied fitting models are within the experimental accuracy of the data, the four-parameter model of Pässler shows the best overlap between estimated data from the fitting parameters, experimental data and data in the literature.

References

- [1] Nadenau V, Hariscos D and Schock H-W 1997 *14th Euro. Photovoltaic Sol. Energy Conf. (Barcelona, Spain, 1997)* p 1250
- [2] Saad M, Riazi H, Bucher E and Lux-Steiner M Ch 1996 *Appl. Phys. A* **62** 181
- [3] Bloss W H, Kimmerle J, Pfisterer F and Schock H W 1984 *Proc. 17th IEEE Photovoltaic Sol. Energy Conf. (New York: IEEE)* p 715
- [4] Schön J H, Baumgartner F P, Arushanov E, Riati-Nejad H, Kloc Ch and Bucher E 1996 *J. Appl. Phys.* **79** 6961
- [5] Mudryi A V, Bodnar I V, Gremenok V F, Viktorov I A, Patuk A I and Shakin I A 1998 *Sol. Energy Mater. Sol. Cells* **53** 247
- [6] Yoshino K, Sugiyama M, Maruoka D, Chichibu S F, Komaki H, Umeda K and Ikari T 2001 *Physica B* **302/303** 357
- [7] Bauknecht A, Siebentritt S, Albert J, Tomm Y and Lux-Steiner M Ch 2000 *Japan. J. Appl. Phys.* **39** (Suppl.) 322
- [8] Chichibu S, Harada Y, Uchida M, Wakiyama T, Matsumoto S, Shirakata S, Isomura S and Higuchi H 1994 *J. Appl. Phys.* **76** 3009

- [9] Yamada A, Makita Y, Niki S, Obara A, Fons P, Hajime H, Kawai M, Chichibu S and Nakanishi H 1996 *J. Appl. Phys.* **79** 4318
- [10] Schön J H, Schenker O, Kulyuk L L, Frimelt K, Kloc Ch and Bucher E 1998 *Sol. Energy Mater. Sol. Cells* **51** 371
- [11] Chichibu S, Mizutani T, Murakami K, Shioda T, Kurafuji T, Nakanishi H, Niki S, Fons P J and Yamada A 1998 *J. Appl. Phys.* **83** 3678
- [12] Bauknecht A, Siebentritt S, Albert J and Lux-Steiner M Ch 2001 *J. Appl. Phys.* **89** 4391
- [13] Meeder A, Fuertes Marrón D, Chu V, Conde J P, Jäger-Waldau A, Rumberg A and Lux-Steiner M Ch 2002 *Thin Solid Films* **403/404** 493
- [14] Yoshino K, Maruoka D, Ikari T, Fons P J, Niki S and Yamada A 2000 *Appl. Phys. Lett.* **77** 259
- [15] O'Donnell K P and Chen X 1991 *Appl. Phys. Lett.* **58** 2924
- [16] Varshni Y P 1967 *Physica* **34** 149
- [17] Yang Z, Homewood K P, Finney M S, Harry M A and Reeson J 1995 *J. Appl. Phys.* **78** 1958
- [18] Pässler R 1997 *Phys. Status Solidi b* **200** 155
- [19] Giannini C, Lagomarsino L, Scarinci F and Castrucci P 1992 *Phys. Rev. B* **45** 882
- [20] Wada M, Araki S, Kudou T, Umezawa T and Nakajima S 2000 *Appl. Phys. Lett.* **76** 2722
- [21] Rincon C, Wasim S M, Marin G, Marquez R, Nieves L and Sanchez-Perez G 2001 *J. Appl. Phys.* **90** 4423
- [22] Pankove J I 1975 *Optical Processes in Semiconductors* (New York: Dover)
- [23] Meeder A, Fuertes Marrón D, Tezlevan V, Arushanov E, Rumberg A, Schedel-Niedrig T and Lux-Steiner M Ch 2003 *Thin Solid Films* **431/432** 214
- [24] Yu P Y and Cardona M 1996 *Fundamentals of Semiconductors—Physics and Material Properties* (Berlin: Springer)
- [25] Wasim S M, Rincón C, Marin G, Bocaranda P, Hernández E, Bonalde I and Medina E 2001 *Phys. Rev. B* **64** 195101
- [26] Neumann H, Hörig W, Reccius E, Möller W and Kühn G 1978 *Solid State Commun.* **27** 449
- [27] Schuler S, Nishiwaki S, Beckmann J, Rega J, Brehme S, Siebentritt S and Lux-Steiner M Ch 2002 *29th IEEE Photovoltaic Specialist Conf. (IEEE, New Orleans, 2002)*
- [28] Siebentritt S and Schuler S 2003 *J. Phys. Chem. Solids* at press
- [29] Rincon C and Ramirez F J 1992 *J. Appl. Phys.* **72** 4321
- [30] Bodnar I V, Karoza A G and Smirnova G F 1977 *Phys. Status Solidi b* **84** K65